Journal of Computational and Applied Mathematics 233 (2010) 2081–2089

Contents lists available at ScienceDirect

Journal of Computational and Applied Mathematics

journal homepage: www.elsevier.com/locate/cam

A numerical approach for solving an extended Fisher–Kolomogrov–Petrovskii–Piskunov equation

S.A. Khuri *, A. Sayfy

Department of Mathematics and Statistics, American University of Sharjah, United Arab Emirates

ARTICLE INFO

Article history:
Received 26 October 2008
Received in revised form 21 September 2009

Keywords:
Fisher–Kolomogrov–Petrovskii–Piskunov equation
Finite differences
B-spline collocation
Integro-differential equation
Composite weighted trapezoidal rule

ABSTRACT

In the present paper a numerical method, based on finite differences and spline collocation, is presented for the numerical solution of a generalized Fisher integro-differential equation. A composite weighted trapezoidal rule is manipulated to handle the numerical integrations which results in a closed-form difference scheme. A number of test examples are solved to assess the accuracy of the method. The numerical solutions obtained, indicate that the approach is reliable and yields results compatible with the exact solutions and consistent with other existing numerical methods. Convergence and stability of the scheme have also been discussed.

1. Introduction

The aim of the paper is dedicated for seeking a numerical solution of the generalized Fisher–Kolomogrov–Petrovskii–Piskunov, FKPP, equation subject to specified initial and boundary conditions given by:

$$u_t(x,t) = q(x,t) + f(u) + \lambda u_x(x,t) + \mu u_{xx}(x,t) + \frac{D}{\tau}\int_0^t \mathrm{e}^{-\frac{t-s}{\tau}} \quad u_{xx}(x,s)\mathrm{d}s, \tag{1.1}$$

where $(x,t) \in (a,b) \times (0,\infty)$. The equation is coupled with the initial condition

$$u(x,0) = p(x), \tag{1.2}$$

and the boundary conditions

$$\begin{aligned} \alpha_0 u(a,t) + \beta_0 u_x(a,t) &= r_0(t), \\ \alpha_1 u(b,t) + \beta_1 u_x(b,t) &= r_1(t), \end{aligned} \tag{1.3}$$

where $t > 0$. Here $u(x,t)$ is the unknown function to be determined, and $p(x)$, $q(x,t)$, $r_0(t)$, and $r_1(t)$ are prescribed functions. Furthermore, α_0, α_1, β_0, β_1, λ, μ, D, and τ are given constants. The function $f(u)$ is a linear or nonlinear function in u.

The integro-differential equation (1.1), a prototypical reaction–diffusion equation, arises in a substantial number of biological and chemical phenomena. Reaction-transport systems with memory and long range interaction in some biological applications were modeled by FKPP equation. The equation was first suggested as a deterministic version of a stochastic model for the spatial spread of a favored gene in a population.

* Corresponding author.
E-mail address: skhoury@aus.edu (S.A. Khuri).

0377-0427/$ – see front matter © 2009 Elsevier B.V. All rights reserved.
doi:10.1016/j.cam.2009.09.041

In recent years, several analytical and numerical studies for integro-differential equations of type (1.1), complimented with conditions of the form (1.2)–(1.3), arise in the literature. A number of numerical algorithms, such as splitting technique and method of lines, are available for obtaining approximate solutions of the FKPP problem as well as other nonlinear partial differential equations [1]. For instance, Branco et al. [2] considered the method of lines approach for numerically solving the Fisher–Kolomogrov–Petrovskii–Piskunov equation. Araújo et al. [3] studied the qualitative properties of the solution of Eq. (1.1), with given initial and Dirichlet boundary conditions, as well as the stability of the model. Splitting methods were introduced to compute numerical approximations presenting the qualitative behavior of the solutions. Other papers considered particular cases of the general model (1.1)–(1.3), for example, Araújo et al. [4] studied the qualitative properties of numerical traveling wave solutions for integro-differential equations, which generalize the well known Fisher equation. The integro-differential equation was replaced by an equivalent hyperbolic equation which allows them to characterize the numerical velocity of traveling wave solutions. Numerical results were presented. In [5], Araújo et al. studied the effect of integral memory terms in the behavior of diffusion phenomena. The energy functional associated with different models was analyzed and stability inequalities were established. Approximation methods for the computation of the solution of the integro-differential equations were constructed. In [6], Barbeiro and Ferreira proposed new mathematical models for percutaneous absorption of a drug. The new models are established by introducing, in the classical Fick's law, a memory term being the advection–diffusion equations of the classical models replaced by integro-differential equations. The well-posedness of the models was studied with Dirichlet, Neumann and natural boundary conditions. Methods for the computation of numerical solutions were proposed. Stability and convergence of the introduced methods were studied, and numerical simulations illustrating the behavior of the model were included. For more details on other analytical and numerical approaches in the literature, see the references in papers [3–6].

In this paper, a numerical method based on finite differences, composite weighted trapezoidal rule, and B-splines is introduced for the numerical solution of a generalized form of the FKPP integro-differential equation (1.1) subject to the mixed boundary conditions (1.3) and the initial condition (1.2). The spline collocation method (see [7–10] and the references therein) is often used for solving nonlinear problems that arise in the physical applications. The performance of the numerical scheme is assessed with some specific test problems; the numerical experiments demonstrate the accuracy and stability of the collocation finite element scheme.

The paper is organized as follows. In Section 2, the numerical method is discussed for the solution of the extended FKPP integro-differential problem. In Section 3, numerical examples are included to assess and illustrate the method. In Section 4, a conclusion is given that briefly summarizes the numerical outcomes.

2. The numerical method

In this section, the finite element approach is presented to obtain a numerical solution to the parabolic problem given by Eqs. (1.1)–(1.3).

To construct such a numerical solution, we first consider the nodal points (x_j, t_m) defined in the region $[a, b] \times [0, T]$ where

$$a = x_0 < x_1 < \cdots < x_{n-1} < x_n = b, \quad x_{j+1} - x_j = h,$$

and

$$0 = t_0 < t_1 < \cdots < t_m < \cdots < T, \quad t_{i+1} - t_i = k.$$

In such a case we have $x_j = a + jh$ for $j = 0, 1, 2, \ldots, n$, and $t_m = mk$ for $m = 0, 1, 2, \ldots$.

The initial condition in (1.2) is approximated as follows:

$$u(x, 0) = p(x) = u(x, t_0), \quad a \le x \le b. \tag{2.4}$$

Denoting $u_m = u(x, t_m)$, the initial condition can be rewritten as

$$u_0 = p(x). \tag{2.5}$$

Next, the 2-point backward differentiation formula is manipulated to approximate u_t, given in Eq. (1.1), at the time-level t_{m+1} for $m = 0, 1, 2, \ldots$. Therefore, we have

$$\begin{aligned} &\frac{u_{m+1} - u_m}{k} = q(x, t_{m+1}) + f(u_{m+1}) + \lambda u^{(1)}_{m+1} + \mu u^{(2)}_{m+1} + \\ &\frac{D}{\tau} \int_0^{t_{m+1}} \mathrm{e}^{-\frac{t_{m+1}-s}{\tau}} u^{(2)}(x, s)\mathrm{d}s. \end{aligned} \tag{2.6}$$

Equivalently, we can rewrite this equation as

$$u_{m+1} - kf(u_{m+1}) - \lambda k u^{(1)}_{m+1} - \mu k u^{(2)}_{m+1} - \frac{Dk}{\tau} \int_0^{t_{m+1}} \mathrm{e}^{-\frac{t_{m+1}-s}{\tau}} u^{(2)}(x, s)\mathrm{d}s = u_m + kq(x, t_{m+1}). \tag{2.7}$$

Table 1
ψ_i, ψ_i', and ψ_i'' evaluated at the nodal points.

Nodes	ψ_i	ψ_i'	ψ_i''
x_i	0	0	0
x_{i+1}	1	$\frac{3}{h}$	$\frac{6}{h^2}$
x_{i+2}	4	0	$-\frac{12}{h^2}$
x_{i+3}	1	$-\frac{3}{h}$	$\frac{6}{h^2}$
x_{i+4}	0	0	0

The latter integral will be handled numerically using the composite weighted trapezoidal rule given by:

$$\int_{t_0}^{t_{m+1}} g(s)\mathrm{d}s \simeq k\sum_{i=0}^{m}[wg(t_i)+(1-w)g(t_{i+1})]$$
$$= k\left[wg(t_0)+(1-w)g(t_{m+1})+\sum_{i=1}^{m}g(t_i)\right]. \tag{2.8}$$

Therefore, using (2.8) we get

$$\int_0^{t_{m+1}} \mathrm{e}^{-\frac{t_{m+1}-s}{\tau}}u^{(2)}(x,s)\mathrm{d}s \simeq k\left[w\mathrm{e}^{-(m+1)k/\tau}u_0^{(2)}+(1-w)u_{m+1}^{(2)}+\sum_{i=1}^{m}\mathrm{e}^{-\mathrm{i}k/\tau}u_{m+1-i}^{(2)}\right]. \tag{2.9}$$

Substituting the approximation (2.9) into Eq. (2.7) we have

$$u_{m+1}-kf(u_{m+1})-\lambda k u_{m+1}^{(1)}-\mu k u_{m+1}^{(2)}-\frac{Dk^2}{\tau}\left[w\mathrm{e}^{-(m+1)k/\tau}u_0^{(2)}+(1-w)u_{m+1}^{(2)}+\sum_{i=1}^{m}\mathrm{e}^{-\mathrm{i}k/\tau}u_{m+1-i}^{(2)}\right]$$
$$= u_m+kq(x,t_{m+1}). \tag{2.10}$$

Let $S_m(x)$ be a function that approximates $u(x,t_m)$ for the time-level $t_m=mk$, and is a linear combination of $n+3$ shape functions which is expressed as:

$$S_m(x)=\sum_{i=-3}^{n-1}a_{im}\psi_i(x), \tag{2.11}$$

where $\{a_{im}\}_{i=-3}^{n-1}$ are the unknown real coefficients, to be evaluated, and the $\psi_i(x)$ are the cubic B-spline functions defined by

$$\psi_i(x)=\frac{1}{h^3}\begin{cases}(x-x_i)^3, & [x_i,x_{i+1}]\\ h^3+3h^2(x-x_{i+1})+3h(x-x_{i+1})^2-3(x-x_{i+1})^3, & [x_{i+1},x_{i+2}]\\ h^3+3h^2(x_{i+3}-x)+3h(x_{i+3}-x)^2-3(x_{i+3}-x)^3, & [x_{i+2},x_{i+3}]\\ (x_{i+4}-x)^3, & [x_{i+3},x_{i+4}]\\ 0, & \text{otherwise.}\end{cases} \tag{2.12}$$

From (2.12), the values of ψ_i, ψ_i' and ψ_i'' at the node points x_j, $j=0,1,\ldots,n$ are given according to Table 1.

The approximate solutions $u_m(x)$ for different time-levels are determined iteratively as follows:

Starting with the time-level $t_0=0$, the value of $u_0(x_j)$ and $u_0^{(2)}(x_j)$, for $j=0,1,2,\ldots,n$ are found from Eq. (2.5), and the 3-points differentiation formulas, respectively.

Next, we will approximate the solution u_{m+1} for $m=0$ in Eq. (2.7) by the shape functions S_1, as is given in (2.11). Hence Eq. (2.7) is approximated by:

$$S_1-kf(S_1)-\lambda kS_1^{(1)}-\mu kS_1^{(2)}-\frac{Dk^2}{\tau}\left[w\mathrm{e}^{-k/\tau}u_0^{(2)}+(1-w)S_1^{(2)}\right]=u_0+kq(x,t_1). \tag{2.13}$$

Replacing S_1 by the approximate solution given by (2.11) yields the following nonlinear system of $n+1$ equations:

$$\sum_{i=-3}^{n-1}a_{i1}\psi_i(x_j)-kf\left(\sum_{i=-3}^{n-1}a_{i1}\psi_i(x_j)\right)-\lambda k\sum_{i=-3}^{n-1}a_{i1}\psi_i'(x_j)-\mu k\sum_{i=-3}^{n-1}a_{i1}\psi_i''(x_j)$$
$$-\frac{Dk^2}{\tau}(1-w)\sum_{i=-3}^{n-1}a_{i1}\psi_i''(x_j)=u_0(x_j)+\frac{Dk^2}{\tau}w\mathrm{e}^{-k/\tau}u_0^{(2)}(x_j)+kq(x_j,k). \tag{2.14}$$

To find the $n+3$ coefficients a_{i2}, $i=-3,-2,\ldots,n-1$, two more equations are needed. The conditions in (1.3) give the following two equations:

For $\alpha_0 u(a,t)+\beta_0 u_x(a,t)=r_0(t)$ we have

$$\sum_{i=-3}^{n-1} a_{i1}\left(\alpha_0\psi_i(x_0)+\beta_0\psi_i'(x_0)\right)=r_0(k). \tag{2.15}$$

For $\alpha_1 u(b,t)+\beta_1 u_x(b,t)=r_1(t)$ we have

$$\sum_{i=-3}^{n-1} a_{i1}\left(\alpha_1\psi_i(x_n)+\beta_1\psi_i'(x_n)\right)=r_1(k). \tag{2.16}$$

Upon solving the system of equations (2.14)–(2.16), the function $u_1(x)$ is approximated by the sum:

$$u_1(x_j)=\sum_{i=-3}^{n-1} a_{i1}\psi_i(x_j),\quad j=0,1,2,\ldots,n. \tag{2.17}$$

Next, we find the approximate solutions at time-levels $t_2, t_3, \ldots$ recursively by solving the following system (2.18)–(2.20) for $m=2,3,\ldots$.

$$\sum_{i=-3}^{n-1} a_{i,m}\psi_i(x_j)-kf\left(\sum_{i=-3}^{n-1} a_{i,m}\psi_i(x_j)\right)-\lambda k\sum_{i=-3}^{n-1} a_{i,m}\psi_i'(x_j)-\mu k\sum_{i=-3}^{n-1} a_{i,m}\psi_i''(x_j)$$
$$-\frac{Dk^2}{\tau}(1-w)\sum_{i=-3}^{n-1} a_{i,m}\psi_i''(x_j)=u_{m-1}(x_j)+\frac{Dk^2}{\tau}\sum_{i=1}^{m-1}\mathrm{e}^{-\mathrm{i}k/\tau}u_{m-i}^{(2)}(x_j)+\frac{Dk^2}{\tau}w\mathrm{e}^{-mk/\tau}u_0^{(2)}(x_j)+kq(x_j,mk), \tag{2.18}$$

$$\sum_{i=-3}^{n-1} a_{i,m}\left(\alpha_0\psi_i(x_0)+\beta_0\psi_i'(x_0)\right)=r_0(mk), \tag{2.19}$$

$$\sum_{i=-3}^{n-1} a_{i,m}\left(\alpha_1\psi_i(x_n)+\beta_1\psi_i'(x_n)\right)=r_1(mk). \tag{2.20}$$

The values of $\psi_i(x_j)$, $\psi_i'(x_j)$, and $\psi_i''(x_j)$ at the node points x_j, $j=0,1,\ldots,n$ are determined from Table 1.

The system of equations in (2.18)–(2.20) can be written in matrix form as follows:

$$\mathbf{Cd}-\mathbf{f}=\mathbf{h}, \tag{2.21}$$

where

$$\mathbf{h}=\begin{bmatrix} r_0(mk) \\ u_{m-1}(x_0)+\frac{Dk^2}{\tau}\sum_{i=1}^{m-1}\mathrm{e}^{-\mathrm{i}k/\tau}u_{m-i}^{(2)}(x_0)+\frac{Dk^2}{\tau}w\mathrm{e}^{-mk/\tau}u_0^{(2)}(x_0)+kq(x_0,mk) \\ u_{m-1}(x_1)+\frac{Dk^2}{\tau}\sum_{i=1}^{m-1}\mathrm{e}^{-\mathrm{i}k/\tau}u_{m-i}^{(2)}(x_1)+\frac{Dk^2}{\tau}w\mathrm{e}^{-mk/\tau}u_0^{(2)}(x_1)+kq(x_1,mk) \\ \vdots \\ u_{m-1}(x_{n-1})+\frac{Dk^2}{\tau}\sum_{i=1}^{m-1}\mathrm{e}^{-\mathrm{i}k/\tau}u_{m-i}^{(2)}(x_{n-1})+\frac{Dk^2}{\tau}w\mathrm{e}^{-mk/\tau}u_0^{(2)}(x_{n-1})+kq(x_{n-1},mk) \\ u_{m-1}(x_n)+\frac{Dk^2}{\tau}\sum_{i=1}^{m-1}\mathrm{e}^{-\mathrm{i}k/\tau}u_{m-i}^{(2)}(x_n)+\frac{Dk^2}{\tau}w\mathrm{e}^{-mk/\tau}u_0^{(2)}(x_n)+kq(x_n,mk) \\ r_1(mk) \end{bmatrix},$$

$$\mathbf{f} = k\begin{bmatrix} 0 \\ f\left(a_{-3,m} + 4a_{-2,m} + a_{-1,m}\right) \\ f\left(a_{-2,m} + 4a_{-1,m} + a_{0,m}\right) \\ f\left(a_{-1,m} + 4a_{0,m} + a_{1,m}\right) \\ \cdot \\ \cdot \\ \cdot \\ f\left(a_{n-4,m} + 4a_{n-3,m} + a_{n-2,m}\right) \\ f\left(a_{n-3,m} + 4a_{n-2,m} + a_{n-1,m}\right) \\ 0 \end{bmatrix},$$

$$\mathbf{C} = \begin{bmatrix} \alpha_0 - \dfrac{3\beta_0}{h} & 4\alpha_0 & \alpha_0 + \dfrac{3\beta_0}{h} & 0 & 0 & \cdots & 0 \\ q_0 & r_0 & s_0 & 0 & 0 & \cdots & 0 \\ 0 & q_1 & r_1 & s_1 & 0 & \cdots & 0 \\ \cdot & \cdot & \cdot & \cdot & \cdot & \cdot & \cdot \\ \cdot & \cdot & \cdot & \cdot & \cdot & \cdot & \cdot \\ \cdot & \cdot & \cdot & \cdot & \cdot & \cdot & \cdot \\ 0 & 0 & 0 & \cdots & q_n & r_n & s_n \\ 0 & 0 & 0 & \cdots & \alpha_1 - \dfrac{3\beta_1}{h} & 4\alpha_1 & \alpha_1 + \dfrac{3\beta_1}{h} \end{bmatrix},$$

where

$$q_j = 1 + \frac{3\lambda k}{h} - \frac{6\mu k}{h^2}, \qquad r_j = 4 + \frac{12\mu k}{h^2},$$

$$s_j = 1 - \frac{3\lambda k}{h} - \frac{6\mu k}{h^2},$$

and

$$\mathbf{d} = \begin{bmatrix} a_{-3,m} & a_{-2,m} & a_{-1,m} & a_{0m} & \cdots & a_{n-3,m} & a_{n-2,m} & a_{n-1,m} \end{bmatrix}^{\mathrm{T}}.$$

3. Numerical test examples

In this section, the spline collocation method is implemented to obtain numerical solutions for particular cases of the generalized wave equation subject to the non-local conservation condition given in Eqs. (1.1)–(1.3). Five examples are discussed; the numerical results are contrasted with existing numerical solutions or with the exact solution at some nodes x_j for some time-levels t_m using specific space-step h and time-step k.

A computer program, based on the finite element method as described in the previous section, is built using the computer algebra system *Maple* code. The program is then applied to solve the five examples. All the computations are done with 25 significant digits.

Example 1. Consider the following special case of Eq. (1.1) (see example 1 in reference [3]) with reaction term of type $f(u) = u(1-u)$:

$$u_t = u(1-u) - 0.5u_x + 0.1u_{xx} + 10\int_0^t \mathrm{e}^{-\frac{t-s}{0.01}} u_{xx}(x,s)\mathrm{d}s, \tag{3.22}$$

where $(x, t) \in (0, 10) \times (0, 1]$ subject to the initial condition

$$u(x,0) = \begin{cases} 1, & 0 \le x \le 5 \\ 0, & 5 < x \le 10 \end{cases}, \tag{3.23}$$

and the boundary conditions

$$u(0,t) = 1, \qquad u(10,t) = 0, \tag{3.24}$$

where $t \in (0, 1]$.

Fig. 1 shows the numerical solution of equations (3.22)–(3.24), obtained by the finite element approach using space-step $h = 0.2$, time-step $k = 0.005$, and weight $w = 0.5$. The graph shows compatibility with the numerical solution of a similar problem discussed in reference [3] (see Fig. 4 therein).

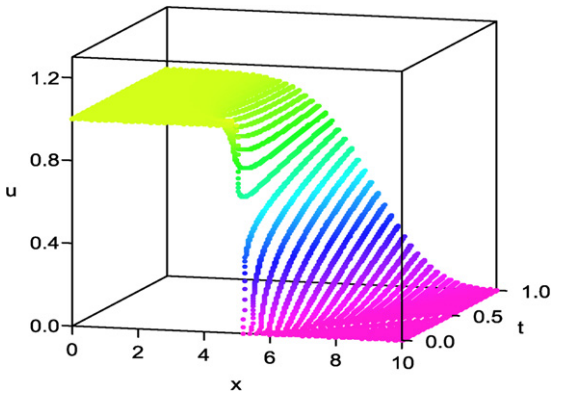

Fig. 1. Numerical solution of Example 1 using $h = 0.2$ and $k = 0.005$.

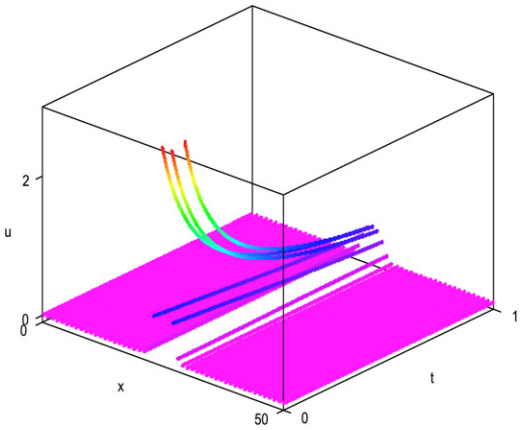

Fig. 2. Numerical solution of Example 2 using $h = 1.0$ and $k = 0.001$.

Example 2. Consider the following equation (see example 2 in [3]):

$$u_t = -2u^2 + 0.1u_{xx} + \int_0^t \mathrm{e}^{-\frac{t-s}{0.1}} u_{xx}(x, s)\mathrm{d}s, \tag{3.25}$$

where $(x, t) \in (0, 50) \times (0, 1]$ subject to the initial condition

$$u(x, 0) = 8.1\mathrm{sech}(x - 25)^2, \tag{3.26}$$

and the Dirichlet homogeneous boundary conditions

$$u(0, t) = 0, \qquad u(50, t) = 0, \tag{3.27}$$

where $t > 0$.

In Fig. 2, the numerical solution for Eqs. (3.25)–(3.27) is plotted, using space-step $h = 1$ and time-step $k = 0.001$. The graph is in good agreement with the figure obtained in example 2 of [3].

Example 3. Consider the following special case of Eq. (1.1) with reaction term of linear type $f(u) = u$:

$$u_t = u - \frac{1}{2}u_x + \frac{3}{2}u_{xx} + \int_0^t \mathrm{e}^{-(t-s)} u_{xx}(x, s)\mathrm{d}s + q(x, t), \tag{3.28}$$

where $(x, t) \in (0, 2\pi) \times (0, 1]$, $q(x, t) = \frac{1}{2}\cos(x + t) - \frac{1}{2}\mathrm{e}^{-t}\sin x + \sin x \cos t$, subject to the initial condition

$$u(x, 0) = \sin x, \tag{3.29}$$

and the Robin boundary conditions

$$u(0, t) = 0, \qquad u(2\pi, t) + u_x(2\pi, t) = \cos t, \tag{3.30}$$

where $t \in (0, 1]$.

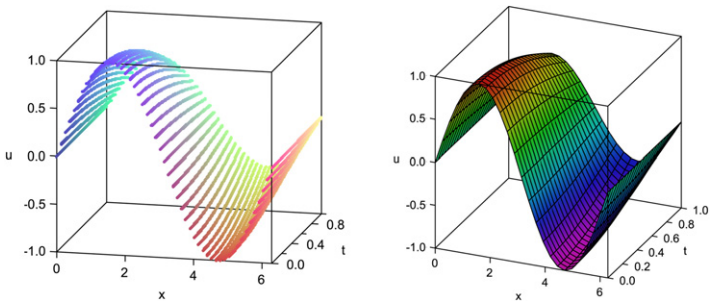

Fig. 3. Numerical and exact solution, respectively, of Example 1 using $h = \pi/25$ and $k = 0.01$.

Table 2
Numerical solution of Example 3 using $h = \pi/25$ and $k = 0.01$.

t	x_0 0.0	x_{10} $2\pi/5$	x_{20} $4\pi/5$	x_{30} $6\pi/5$	x_{40} $8\pi/5$	x_{50} 2π	Max|Error|
0.0	0.000000	0.951057	0.587785	−0.587785	−0.951057	0.000000	0.0
0.1	0.000000	0.945678	0.584443	−0.584472	−0.945667	0.000000	6.7×10^{-4}
0.5	0.000000	0.832128	0.513974	−0.514514	−0.831807	0.001435	2.8×10^{-3}
1.0	0.000000	0.510371	0.314665	−0.316086	−0.509451	0.002763	4.4×10^{-3}

Table 3
Numerical solutions of Example 3 for different values of w.

w	Max|Error|		
	$t = 0.1$	$t = 0.5$	$t = 1.0$
0.1	7.0×10^{-4}	3.4×10^{-3}	5.6×10^{-3}
0.5	6.8×10^{-4}	3.1×10^{-3}	5.0×10^{-3}
0.8	6.7×10^{-4}	2.8×10^{-3}	4.4×10^{-3}

Problem (3.28)–(3.30) has the exact solution $u(x, t) = \sin x \cos t$.

The numerical solution of this problem, using the finite differences spline collocation approach with $h = \pi/25, k = 0.01$ and $w = 0.8$, is recorded for specific mesh points in Table 2 and plotted simultaneously with the exact solution in Fig. 3. The choice of the weight $w = 0.8$ appears to give slightly better numerical solution than other values for w (see Table 3).

From Table 2 and Fig. 3, the finite element approach clearly yields a reliable numerical solution.

Example 4. Consider the following special case of Eq. (1.1) with reaction term of linear type $f(u) = u^2$:

$$u_t = u^2 - \frac{1}{2\pi^2}u_{xx} + \int_0^t \mathrm{e}^{-\frac{t-s}{2}} u_{xx}(x, s)\mathrm{d}s + q(x, t), \tag{3.31}$$

where $(x, t) \in (0, 1) \times (0, 1]$, $q(x, t) = \pi^2 t\mathrm{e}^{-t/2}\sin(\pi x) - \mathrm{e}^{-t}\sin^2(\pi x)$, subject to the initial condition

$$u(x, 0) = \sin(\pi x), \tag{3.32}$$

and the Robin boundary conditions

$$u(0, t) + u_x(0, t) = \pi\mathrm{e}^{-t/2}, \qquad u(1, t) + u_x(1, t) = -\pi\mathrm{e}^{-t/2}, \tag{3.33}$$

where $t \in (0, 1]$.

Problem (3.31)–(3.33) has the exact solution $u(x, t) = \mathrm{e}^{-t/2}\sin(\pi x)$.

In Table 4, the numerical solution for Eqs. (3.31)–(3.32) obtained by the B-spline method at different time-levels, using space-step $h = 0.02$ and time-step $k = 0.005$, and $w = 0.5$, are recorded together with maximum absolute errors. Fig. 4 shows the numerical as well as the exact solution.

From Table 4 and Fig. 4, the B-spline approach clearly yields a reliable numerical solution.

Example 5. Consider the following piecewise-defined problem with reaction term of nonlinear type $f(u) = u^2$:

$$u_t = u^2 + \frac{1}{2\pi^2}u_{xx} + \int_0^t \mathrm{e}^{-\frac{t-s}{2}} u_{xx}(x, s)\mathrm{d}s + q(x, t), \tag{3.34}$$

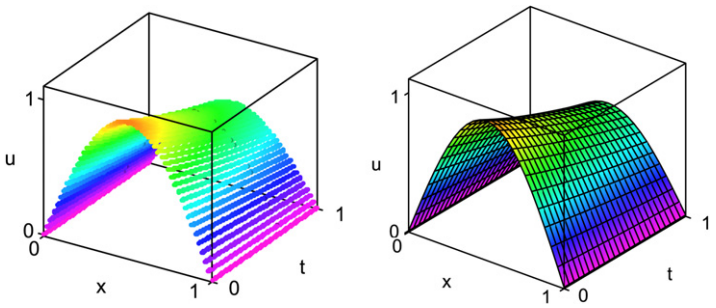

Fig. 4. Numerical and exact solution, respectively, of Example 4 using $h = 0.02$ and $k = 0.005$.

Table 4
Numerical solutions of Example 4 using $h = 0.02$ and $k = 0.005$.

t	x_0 0.0	x_{10} 0.2	x_{20} 0.4	x_{30} 0.6	x_{40} 0.8	x_{50} 1.0	Max|Error|
0.00	0.000000	0.587785	0.951057	0.951057	0.587785	0.000000	0.0
0.01	0.000007	0.559135	0.904703	0.904703	0.559135	0.000005	5.3×10^{-6}
0.50	0.000054	0.457676	0.740530	0.740531	0.457677	0.000044	1.6×10^{-4}
1.00	0.000531	0.355871	0.576128	0.576090	0.355723	0.000889	8.9×10^{-4}

Table 5
Numerical solution of Example 5 using $h = 0.02$ and $k = 0.005$.

t	x_0 0.0	x_{10} 0.2	x_{20} 0.4	x_{30} 0.6	x_{40} 0.8	x_{50} 1.0	Max|Error|
0.00	0.000000	0.587785	0.951057	1.000000	1.000000	1.000000	0.0
0.01	0.000000	0.559219	0.912856	0.993953	0.997847	0.951229	4.8×10^{-2}
0.50	0.000000	0.517887	0.836151	0.844975	0.794156	0.778801	9.6×10^{-2}
1.00	0.000000	0.313192	0.507173	0.532474	0.555864	0.606531	7.5×10^{-2}

where $(x, t) \in (0, 1) \times (0, 1]$, subject to the initial condition

$$u(x, 0) = \begin{cases} \sin(\pi x), & 0 \le x \le 0.5 \\ 1, & 0.5 < x \le 1 \end{cases}, \tag{3.35}$$

and the boundary conditions

$$u(0, t) = 0, \qquad u(1, t) = \mathrm{e}^{-t/2}, \tag{3.36}$$

where $t \in (0, 1]$. Also we have

$$q(x, t) = \begin{cases} \pi^2 t \mathrm{e}^{-t/2} \sin(\pi x) - \mathrm{e}^{-t} \sin^2(\pi x), & 0 \le x \le 0.5 \\ -1, & 0.5 < x \le 1 \end{cases}.$$

Problem (3.34)–(3.36) has the exact solution

$$u(x, t) = \begin{cases} \mathrm{e}^{-t/2} \sin(\pi x), & 0 \le x \le 0.5 \\ \mathrm{e}^{-t/2}, & 0.5 < x \le 1 \end{cases}.$$

In Table 5, the numerical solution for Eqs. (3.34)–(3.36) obtained by the B-spline method at different time-levels, using space-step $h = 0.02$ and time-step $k = 0.005$, are recorded together with maximum absolute errors.

From Table 5 and Fig. 5, the B-spline approach clearly yields a reliable numerical solution.

4. Conclusion

A spline collocation approach was employed for the numerical solution of the extended Fisher–Kolomogrov–Petrovskii–Piskunov equation. The method reduces the underlying problem to a tridiagonal nonlinear system of algebraic equations, which can be solved successively to obtain a numerical solution at varied time-levels. A computer program, based on Maple code and the finite differences spline approach, was developed and then applied to five specific test problems using IBM ThinkPad. The results shown in Tables 2–5 and Figs. 1–5 clearly indicate reliable numerical solutions. Moreover, the results in Tables 6a and 6b confirm that the numerical solutions can be refined when the step-time k is reduced, or the number

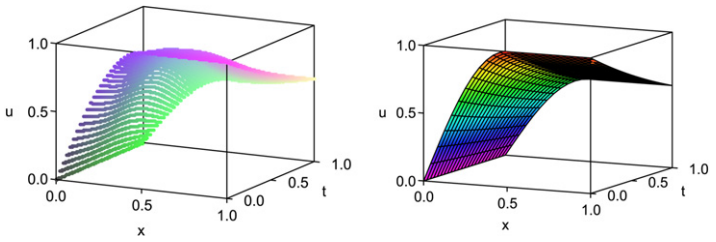

Fig. 5. Numerical and exact solution, respectively, of Example 5 using $h = 0.02$ and $k = 0.005$.

Table 6a
Numerical solutions of Example 4 at time-level $t = 1.0$ using $k = 0.01$.

Number of nodes n	50	40	30	20
Max|Error|	4.4×10^{-3}	5.4×10^{-3}	7.4×10^{-3}	1.3×10^{-2}

Table 6b
Numerical solutions of Example 4 at time-level $t = 1.0$ using $h = \pi/25$.

Time-step k	0.01	0.02	0.04	0.08
Max|Error|	4.4×10^{-3}	7.2×10^{-3}	1.3×10^{-2}	2.8×10^{-2}

of nodes is increased. The results can be further improved slightly via the choice of the weight w such that the integrand values at $x = a$ have more weight than at the right endpoint $x = b$.

It was observed that the accuracy of the numerical results might be affected and the convergence rate degraded if the initial condition is not smooth (see Example 1, where the initial condition is piecewise continuous, and Example 5, where the second derivative is piecewise continuous). Note that in these examples non-smooth conditions decrease the expected rate of convergence; this is expected since the second derivative of the initial value at the node points are approximated by a second-order forward difference formula. The construction of such a second derivative can be accurate if the initial condition is smooth. There are other schemes available, such as averaging the initial data, shifting the grid, and a projection method in conjunction with special time-stepping method, to remedy this problem and handle this limitation in order to achieve convergence and/or higher accuracy, depending on the type of smoothness. In general, finite difference methods have a setback when presented with non-smooth initial conditions. As an alternative, we can manipulate finite element analysis rather than relying on finite difference analysis which assumes smooth data. Finite element schemes require less continuity since they are based on the weak (or integrated) form of the differential equation.

It was also noticed that when k is increased for certain examples, the Maple program fails to solve the nonlinear system at specified time-levels. For these cases, the numerical solution might have an unstable behavior. Possible ways to tackle this problem is to use variable time-step or reduce the space-step h, which will be at the expense of increasing the dimension of the nonlinear system.

References

[1] E. Deeba, S.A. Khuri, Nonlinear equations, in: Wiley Encyclopedia of Electrical and Electronics Engineering, vol. 14, John Wiley & Sons, NewYork, 1999, pp. 562–570.
[2] J.R. Branco, J.A. Ferreira, P. de Oliveira, Numerical methods for the generalized Fisher–Kolomogrov–Piskunov–Piskunov equation, Applied Numerical Mathematics 57 (2007) 89–102.
[3] A. Araújo, R. Branco, J.A. Ferreira, On the stability of a class of splitting methods for integro-differential equations, Applied Numerical Mathematics 59 (3–4) (2009) 436–453.
[4] A. Araújo, J.A. Ferreira, P. de Oliveira, Qualitative behavior of numerical traveling waves solutions for reaction-diffusion equations with memory, Applicable Analysis 84 (2005) 1231–1246.
[5] A. Araújo, J.A. Ferreira, P. de Oliveira, The effect of memory terms in diffusion phenomena, Journal of Computational Mathematics 24 (2006) 91–102.
[6] S. Barbeiro, J.A. Ferreira, Integro-differential models for percutaneous drug absortion, International Journal of Computer Mathematics 84 (2007) 451–467.
[7] A.R. Bahadir, Application of cubic B-spline finite element technique to the thermistor problem, Applied Mathematics and Computation 149 (2004) 379–387.
[8] H.N. Caglar, S.H. Caglar, E.H. Twizell, The numerical solution of third-order boundary value problems with fourth-degree B-spline functions, International Journal of Computer Mathematics 71 (1999) 37381.
[9] H.N. Caglar, S.H. Caglar, E.H. Twizell, The numerical solution of fifth-order boundary value problems with sixth-degree B-spline functions, Applied Mathematics Letters 12 (1999) 25–30.
[10] M. Dehghan, Numerical techniques for a parabolic equation subject to an overspecified boundary condition, Applied Mathematics and Computation 132 (2–3) (2002) 299–313.